# Mechanical Strain Analyses in Silicone-Made Aortic Valve

Nicolas Bueno [a,b*], Viktória Stanová [a], Philippe Pibarot [a], Julien Favier [b]

[a] Institut universitaire de cardiologie et de pneumologie de Québec – ULaval, Québec, Canada ;
[b] Laboratoire de Mécanique, Modélisation et Procédés Propres (M2P2), Aix Marseille Univ, CNRS, Centrale Med, M2P2

***Corresponding author:** nicolas.bueno@etu.univ-amu.fr

**Keywords*: in vitro, aortic valve, strain field.***

## 1. Introduction

Aortic valve stenosis is the third most frequent cardiovascular disease in high-income countries [1]. Currently, no medical therapy is available for successfully treating calcific aortic stenosis and the only option is the valve replacement. The design of a bioprosthetic aortic valve (BAV) has a significant impact on its durability. Regions subjected to higher mechanical stress are more susceptible to structural deterioration [2]. Analyzing strain field across valve designs may offer insight into their relative durability. The purpose of this study is to examine the impact of geometry on strain distribution.

## 2. Methods

### *2.1 Valve geometry and manufacturing*

Parametric valve designs by Xu et al. [3] and Thubrikar [4] were combined and modified to suit the constraints of valve manufacturing and adjust the leaflet free edge. A reference 'normal' geometry was based on a commercially available BAV Trifecta 25 mm (Abbott, MN, USA) with inner diameter of 23 mm and eight variations that were obtained by adjusting: diameter, leaflet height, curvatures or thickness. Figure 1a shows all geometries, each named and annotated with its variation from the normal valve. A Python script was used to generate the nine mold designs, which were 3D printed (Lulzbot Inc., ND, USA) and filled with silicone (DragonSkin30, Smooth-On, Inc., PA, USA). Each valve included a 3D-printed stent mimicking the one of Trifecta valve.

### *2.2 In vitro testing*

Custom made silicone valves were tested in a cardiac simulator [4] under following hemodynamic conditions: heart rate was set to 70 bpm, mean aortic pressure to 100 mmHg and stroke volume to 70 ml. Mean pressure gradient (MPG), and Effective orifice area (EOA) were acquired using continuous-wave Doppler (iE33, Philipps Healthcare, USA). Leaflets motion was recorded with two high-speed cameras (FASTCAM Mini AX50, Photron Inc., USA) equipped with 105 mm lenses. To obtain a high contrast stochastic pattern for the use of digital image correlation (DIC), the leaflet surface was applied with a fine speckle pattern using a black tattoo ink (Killer Ink Tattoo., Liverpool, UK). Measurement of deformation was based on 3D DIC conducted with commercial system VIC3D (Correlated Solutions, Inc, SC, USA). This approach allowed the 3D reconstruction of the valve leaflets deformation during the closure (diastole). The degree of pinwheeling index is evaluated by tracing the contour of a coaptation line and comparing it to the unconstrained, ideal configuration (theoretically straight line) for each valve (expressed as a percentage). This measurement is performed for each half free edge, 0.2 seconds after leaflet closure, and the average is then calculated.

## 3. Results and discussion

Table 1 shows the mean values of the hemodynamic measurements (MPG and EOA), pinwheeling index at 0.2 seconds and the maximum value of the first principal Lagrangian strain ($e_1$) during diastole for the Trifecta valve and the nine silicone valves. It is important to note that strain data were limited to regions of the leaflets that were simultaneously visible from both cameras and remained within the field of view throughout the cycle. As a result, the reported strain values represent the maximum within these analyzable regions. Figure 1b shows the first principal Lagrange strain (e1) for each silicone aortic valve 0.2 second after leaflet coaptation (valve fully closed). Higher deformations were consistently observed near the commissures. Thicker leaflets (valves *th_diff* and *th1*) exhibited reduced deformation ($e_1\, max = 0.54$ and 0.60 respectively), while the valve with the smallest diameter (*d21*) showed a localized high deformation at one commissure ($e_1$ = 1.25). Valve *x2*, characterized by an increased free edge angle relative to the horizontal, showed the lowest overall deformation ($e_1 max = 0.51$). Valve *x1* showed a strong inward pulling in the stent posts regions, likely due to the increased distance between leaflets, requiring more tissue stretching during closure. Finally, valve *h16* exhibited visible pinwheeling (4.89±2.42%), due to excess leaflet tissue. Pinwheeling decreased as a result of a decrease in leaflet height, as demonstrated by the normal and *h12* valves, which had progressively shorter leaflets.

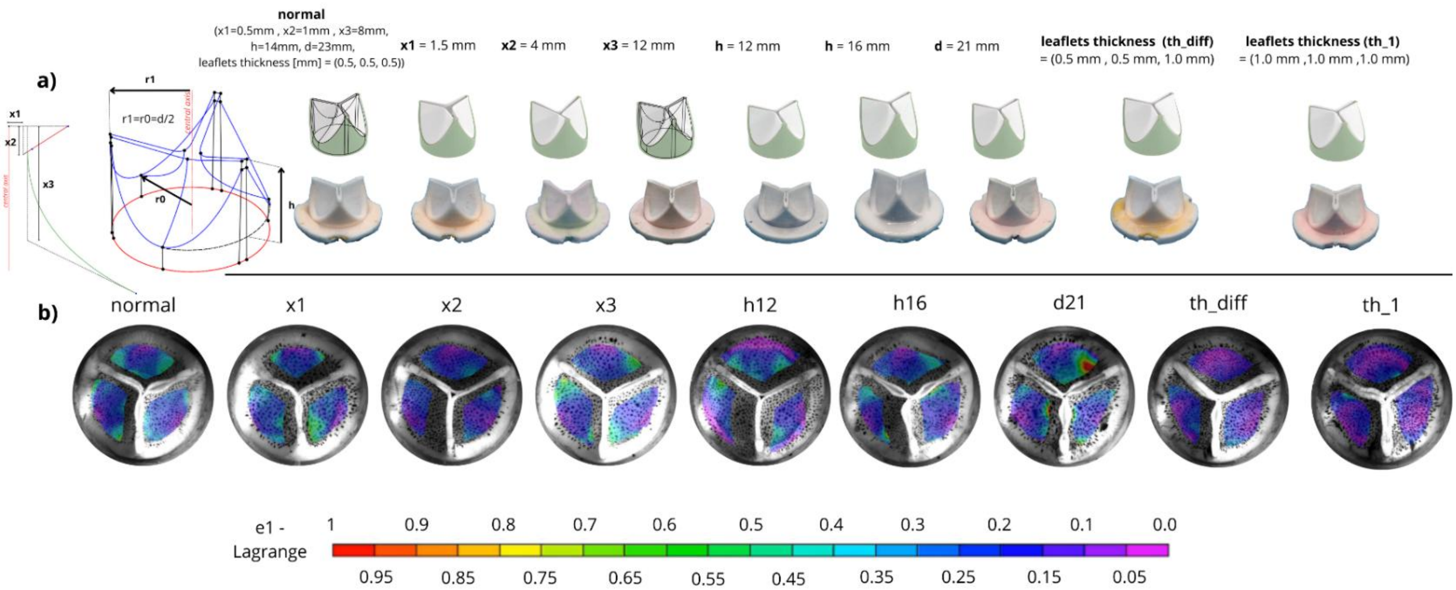


***Figure 1.*** *(a) : Geometric construction of the valve, 3D model and silicone valve for 9 tested valves. (b) First principal Lagrange strain field (e1) for the 9 tested valves 0.2 s after closure. To enable comparison, the same color scale was used for all strain fields, despite varying minimum and maximum values across valves.*

| | *MPG (mmHg)* | *EOA* ($cm^2$) | *Pinwheeling* | $e_1 max$ |
|---|---|---|---|---|
| *Trifecta* | *6.08±0.23* | *2.15* | *0.81±0.64* | *0.35* |
| *normal* | *6.37±0.21* | *2.12* | *3.82±2.54* | *0.72* |
| *x1* | *6.47±0.20* | *2.12* | *1.24±1.73* | *0.80* |
| *x2* | *6.46±0.10* | *2.26* | *0.79±0.76* | *0.51* |
| *x3* | *8.05±0.25* | *1.75* | *0.86±1.03* | *0.89* |
| *h12* | *5.71±0.42* | *2.25* | *1.19±1.49* | *1.09* |
| *h16* | *5.11±0.22* | *2.43* | *4.89±2.42* | *1.01* |
| *d21* | *7.82±0.22* | *1.92* | *4.55±1.63* | *1.25* |
| *th_diff* | *12.54±0.84* | *1.50* | *2.22±1.71* | *0.54* |
| *th_1* | *14.75±0.74* | *1.23* | *3.09±2.40* | *0.60* |

***Table 1.*** *Mean pressure gradient (with standard deviation), effective orifice area, pinwheeling (with standard deviation) and first principal Lagrangian strain for Trifecta valve and each silicone valve*

## 4. Conclusions

The results of this study demonstrate that silicone valves can be used to evaluate the impact of geometric parameters on leaflet strain fields in BHVs. Valve *x2* presented the lowest strain level and its hemodynamic performance during systole was favorable, as shown in Table 1. However, to confirm the benefit of this geometric feature, the coaptation area of valve *x2* should also be evaluated. Valve *x3*, with increased belly curvature, shows favorable strain behavior but demonstrated poor systolic opening and inferior hemodynamic performance compared to most other geometries, due to excess tissue in the belly region.

This experimental method across different geometries enables the investigation of how specific valve design features influence tissue strain. This method contributes to identifying which features are more likely to promote calcification and leaflet tear, and to localize regions most susceptible to its initiation.
This approach could also be applied to native valves with patient-specific geometries and pathological conditions. It is possible to incorporate calcifications into silicone valve models to experimentally evaluate their mechanical impact.
Although the silicone material used result in greater deformation than in biological valves, this model remains relevant for comparing geometric effects.

## Conflict of Interest Statement

Pr. Philippe Pibarot reports research grants from Edwards Lifesciences, Medtronic, and Pi-Cardia.
All other authors have no conflict of interest to disclose

## References

1. Roth, G.A., et al., *Global burden of cardiovascular diseases and risk factors, 1990-2019: update from the GBD 2019 study.* J Am Coll Cardiol, 2020. **76**(25): p. 2982-3021.
2. Vesely, I., *The evolution of bioprosthetic heart valve design and its impact on durability.* Cardiovasc Pathol, 2003. **12**(5): p. 277-86.
3. Fei Xu, et al. *A framework for designing patient-specific bioprosthetic heart valves using immersogeometric fluid–structure interaction analysis.* 2017.

4. Thubrikar, M., *The Aortic Valve*. 2018.